

Photovoltaic properties and inner electric field of ZnO/Zn-phthalocyanine hybrid solar cells

Yuki Yoshida ^a, Makoto Nakamura ^a, Senku Tanaka ^b, Ichiro Hiromitsu ^{a,*},
Yasuhisa Fujita ^c and Katsumi Yoshino ^{d, e}

^a *Department of Material Science, Faculty of Science and Engineering, Shimane University, Matsue 690-8504, Japan*

^b *Center for Integrated Research in Science, Shimane University, Matsue 690-8504, Japan*

^c *Department of Electronic and Control Systems Engineering, Shimane University, Matsue 690-8504, Japan*

^d *Research Project Promotion Institute, Shimane University, Matsue 690-8504, Japan*

^e *Center for Advanced Science and Innovation, Osaka University, Suita 565-0871, Japan*

* Corresponding author. Tel.: +81-852-32-6391; fax: +81-852-32-6409

E-mail address: hiromitu@riko.shimane-u.ac.jp (I. Hiromitsu)

Abstract

The photovoltaic properties and distribution of inner electric field were studied for ZnO/Zn-phthalocyanine(ZnPc)/Au solar cells, the ZnO films of which were prepared by the metal organic chemical vapor deposition (MOCVD) method. The photocurrent is generated only by the excitation of ZnO, and the excitation of ZnPc does not contribute to the photocurrent generation. An electroabsorption (EA) study indicated that the inner electric field only exists in the ZnO layer. The absence of the inner electric field in the ZnPc layer results in the absence of photocurrent with ZnPc excitation.

Keywords: Solar cells; Zinc oxide; Organic semiconductors; Phthalocyanine; Electroabsorption; Chemical vapor deposition (CVD)

1. Introduction

Organic thin-film solar cells have been extensively studied as candidates for practical devices based on organic semiconductors. One of the important issues regarding the mechanism of the photovoltaic effect is the role of the inner electric field in carrier generation. It had been thought that, in the case of organic semiconductors, the inner electric field could not contribute to the dissociation of the excitons because the exciton binding energy of organic semiconductors is generally high compared to that of inorganic semiconductors [1,2]. However, we have recently shown by electroabsorption (EA) studies of the inner electric field that the dissociation of the excitons is caused by the inner electric field in several types of phthalocyanine-based organic thin-film solar cells [3-5].

In the present paper, the study is extended to organic–inorganic hybrid solar cells made of Zn-phthalocyanine (ZnPc) and ZnO which are *p*- and *n*-type semiconductors, respectively. The hybridization of organic and inorganic semiconductors in solar cells may possibly be a breakthrough to obtain higher conversion efficiency. Several types of ZnO-based hybrid solar cells have been reported by several groups [6-12]. However, the effect of hybridization on the distribution of the inner electric field has not been reported. In order to understand the photovoltaic mechanism in the hybrid solar cells, study of the inner electric field is important. Here, we study the photovoltaic properties and the inner electric field of a ZnO/ZnPc/Au system. The features of the distribution of the inner electric field are significantly different from those of pure organic cells.

2. Experimental

Zn-phthalocyanine (ZnPc) was purchased from Kanto Chem. Co., Inc. and was used after three sublimations in a vacuum. Au of 99.95 % purity was purchased from Nilaco Corp.

ZnO films were prepared by MOCVD method [13] using a HR-1202 apparatus from Nippon Sanso Corp. Diisopropylzinc (*Di-PrZn*) and tertiary butanol (*t-BuOH*) were used as the precursors for ZnO, and were introduced into the reactor with hydrogen carrier gas. The VI/II ratio, the ratio of the number of oxygen atoms to that of Zn in the precursor materials, was 90 or 10. ZnO was grown on quartz substrates of $10 \times 10 \times 0.5$ mm³ which were placed on a susceptor kept at 350 °C. The pressure in the MOCVD chamber was kept at 1×10^{-4} Pa. The ZnO film obtained had a sheet resistance of about 5 and 10 k Ω/\square for VI/II = 90 and 10, respectively. The film thickness of the ZnO film for VI/II = 90 could be estimated to be ~200 nm from the interference peaks in the optical absorption spectrum.

The arrangement of the thin films in the ZnO/ZnPc/Au sandwich cell is shown in Fig. 1. On the ZnO film, thin films of ZnPc and Au were evaporated under a pressure of 1×10^{-4} Pa. The film thickness was 140 nm for ZnPc and 15 nm for Au. The speed of the evaporation was 0.1 nm/s for ZnPc and 0.02 nm/s for Au. The effective area of the device is 0.3 cm².

Photoluminescence (PL) spectra were measured at 15 K using a He-Cd laser (325 nm) for optical pumping. Photocurrent action spectra were measured at room temperature using a 300 W xenon lamp as a light source followed by a monochromator.

The inner electric field was studied by EA technique at room temperature, in which electric-field modulation was applied to the device and a synchronous change in the optical absorption coefficient was detected [3,4]. The electric circuit for the EA measurement is shown in Fig. 1. An electric-field modulation of 1 Hz was applied to the device using a function generator whose output signal was $V_m \sin \omega_m t$ with $V_m = 0.5$ V. The probe light entered normally into the active area of the device from the quartz side. The light source was a 100 W halogen lamp followed by a monochromator. The transmitted light intensity, T , was detected by a photomultiplier tube. The amplitude of the change in the transmitted light intensity, ΔT , with frequency ω_m was detected by a lock-in amplifier. Then, $-\Delta T/T$ is proportional to the change in the optical absorption coefficient and has the following relationship [3,14].

$$-\frac{\Delta T}{T} = \sum_{i=1}^2 E_{0i} E_{mi} d_i \text{Im} \chi_i^{(3)}, \quad (1)$$

where E_{0i} , E_{mi} , d_i and $\text{Im} \chi_i^{(3)}$ are the static inner electric field, the amplitude of the modulation electric field, the film thickness and the imaginary part of the third-order electric susceptibility, respectively, of the i th layer, where $i = 1$ and 2 correspond to the ZnO and ZnPc layers, respectively.

3. Results and discussion

3-1. Photoluminescence of the ZnO films

Figure 2 shows the PL spectra at 15 K of the two ZnO films prepared with VI/II

ratios of 90 and 10. The two peaks at 369 and 374 nm are assigned to the donor-bound excitons (D^0X) and acceptor-bound excitons (A^0X), respectively [13,15]. The spectra are dominated by the D^0X line. Therefore, the present ZnO films show a n -type luminescence.

Comparing the two spectra in Fig. 2, the PL intensity for VI/II = 90 is only 1/80 of that for VI/II = 10. This indicates that the dissociation of the excitons occurs rapidly for VI/II = 90 probably due to the existence of unknown impurities or defects that quench the luminescence.

3-2. J - V characteristics

Figure 3(a) shows the bias dependence of the dark current density, J_{dark} , at room temperature of two ZnO/ZnPc/Au cells with the ZnO films prepared under VI/II = 90 and 10. J_{dark} at $V_{\text{bias}} = +2$ V is $94 \mu\text{A}/\text{cm}^2$ for VI/II = 90, and $8 \mu\text{A}/\text{cm}^2$ for VI/II = 10. The rectification ratio at $V_{\text{bias}} = \pm 2$ V is 2000 for VI/II = 90, and 100 for VI/II = 10. Thus, the cell for VI/II = 90 has a much better rectification property. Figure 3(b) shows the bias dependence of the current density, J_{photo} , under an illumination by white light of AM 1.5, $100 \text{ mW}/\text{cm}^2$. The short circuit current density and open circuit voltage for VI/II = 90 are $30 \mu\text{A}/\text{cm}^2$ and 0.27 V, respectively, and those for VI/II = 10 are $0.3 \mu\text{A}/\text{cm}^2$ and 0.15 V. Thus, the cell for VI/II = 90 has much better photovoltaic properties compared to the cell for VI/II = 10. As will be shown in the next subsection, most of the photocurrent is generated by the photoexcitation of ZnO. The better photovoltaic properties for VI/II = 90 may be related to the larger number of impurities or defects in

the ZnO layer suggested by the weaker PL intensity for VI/II = 90, because the impurities and defects may enhance the dissociation of the excitons.

3-3. Photocurrent action spectrum

Figure 4(a) shows the photocurrent action spectra of the ZnO/ZnPc/Au cell for VI/II = 90 measured under $V_{\text{bias}} = 0$ and 0.6 V. The sign of the photocurrent is inverted by applying a bias voltage of 0.6 V in agreement with Fig. 3(b). The action spectrum has a peak in the wavelength range between 330 and 400 nm. Figure 4(b) shows the optical absorption spectra of the ZnO film for VI/II = 90 and the ZnPc film. Comparing Figs. 4(a) and 4(b), it is seen that the photoexcitation of ZnPc has a negligibly small contribution to the photocurrent. Then, the peak at 340 ~ 400 nm in the action spectrum is attributed to ZnO excitation.

3-4. Electroabsorption

Figure 4(c) shows the EA spectra of the ZnO/ZnPc/Au cell for VI/II = 90 measured under $V_{\text{bias}} = 0$ and 0.6 V. Each EA spectrum has sharp peaks in the range between 350 and 400 nm, and is close to the 2nd derivative of the absorption spectrum of ZnO as shown in Fig. 5. Thus, the EA spectra in Fig. 4(c) are attributed to ZnO, and no EA signal is observed from ZnPc. This indicates that the inner electric field exists only in the ZnO layer because the EA signal intensity is proportional to the inner electric field in Eq. (1). The line shape of the EA spectrum close to the 2nd derivative of the absorption spectrum of ZnO indicates that the excitons in the ZnO layer are weakly

bound [16].

The EA signal intensity, V_{EA} , of ZnO is defined in Fig. 5 by the difference between the signal heights at 374.5 and 379.5 nm. The bias dependence of V_{EA} is shown in Fig. 6. For $V_{bias} \leq 0$ V, V_{EA} has a weak bias dependence, while, for $V_{bias} > 0$ V, $|V_{EA}|$ decreases steeply as V_{bias} is increased and almost disappears for $V_{bias} \geq 1.5$ V. On the other hand, J_{photo} in Fig. 3 for VI/II = 90 increases monotonically as V_{bias} is increased and changes its sign at $V_{bias} = 0.25$ V. Thus, the correlation between V_{EA} and J_{photo} is poor. Poor correlation is also seen in a comparison of Figs. 4(a) and 4(c). The sign of the photocurrent action spectrum is inverted by applying a bias of 0.6 V in Fig. 4(a) while the sign of the EA spectrum in Fig. 4(c) is unchanged. The shapes of the photocurrent action spectrum as well as that of the EA spectrum are essentially the same for the two cases of $V_{bias} = 0$ and 0.6 V as seen in Figs. 4(a) and 4(c). This indicates that the photocurrent is generated by the photoexcitation of ZnO but is not correlated with the electric field in the ZnO layer. On the other hand, the absence of the photocurrent with ZnPc excitation is a result of the absence of the inner electric field in the ZnPc layer. This agrees with our previous results that the dissociation of the excitons in the ZnPc layer is caused by the inner electric field [3-5].

For $V_{bias} \geq 1.5$ V, no inner electric field exists either in the ZnO or ZnPc layer. Similar quenching of the inner electric field under the forward bias condition has been reported in some organic solar cells [3-5] and organic light emitting diodes [17,18]. In such cases, the applied bias voltage may be used up as a potential drop at the interfaces by the formation of dipole layers there.

The energy band diagrams proposed from the present results are shown in Fig. 7. The inner electric field is proportional to the slope of the band. For $V_{\text{bias}} = 0$ V, the electric field exists only in the ZnO layer. By the photoexcitation of ZnO, carriers are generated which drift with the inner electric field in the ZnO layer. For $V_{\text{bias}} > 1.5$ V, the band of ZnO as well as that of ZnPc become flat. The carriers are still generated by the photoexcitation of ZnO, and are probably moved by a diffusion process.

The most remarkable point in the present results is that the electric field exists only in the ZnO layer for $V_{\text{bias}} = 0$ V. In our past studies on solar cells made of ZnPc film with a thickness in the order of 100 nm, a finite electric field in the ZnPc layer was always observed by EA for $V_{\text{bias}} = 0$ V. The resistivity of ZnO and ZnPc are in the order of 10^{-1} and 10^6 Ω cm, respectively. Here, the resistivity of ZnO was estimated from the sheet resistance of the ZnO film and that of ZnPc from the resistance of a Au/BCP/ZnPc/BCP/Au sandwich cell, where BCP stands for bathocuproine and was inserted between Au and ZnPc to obtain a better electrical contact [19]. Since the resistivity of ZnPc is much higher than that of ZnO, the expectation is that an electric field of substantial intensity exists in the ZnPc layer. The experimental results contradict this expectation. No degradation nor chemical reaction of ZnPc is detected in the optical absorption spectrum of the cell. The absence of the electric field in the ZnPc layer for $V_{\text{bias}} = 0$ V is explained only by the existence of a large number of trapped negative charges at the surface of the ZnPc layer as shown in Fig. 7(a). These negative charges compensate for the positive charges in the ZnO layer. Thus, the ZnO/ZnPc interface in the present device should be full of charge traps.

In Fig. 7(a), it was assumed that the electric field exists over the whole ZnO layer of ~ 200 nm thickness, in other words, the ZnO layer is totally depleted. This is because the depletion-layer width of the present ZnO film is expected to be substantially larger than 100 nm judging from a report that a ZnO film with a conductivity two-orders higher than the present ZnO film has a depletion-layer width of ~ 100 nm [20].

The magnitudes of the electric field in the ZnO layer for $V_{\text{bias}} = 0$ and 0.6 V are estimated as follows. The built-in potential for the present ZnO layer is roughly estimated to be 0.7 V from the slope of the $V_{\text{EA}} - V_{\text{bias}}$ plot at $V_{\text{bias}} = 0$ V in Fig. 6. Then, the inner electric field of the ZnO layer at $V_{\text{bias}} = 0$ V becomes 3.5×10^4 V/cm. The electric field for $V_{\text{bias}} > 1.5$ V is estimated to be 1.5×10^3 V/cm from the value of V_{EA} in Fig. 6. This corresponds to a voltage drop of 0.03 V across the ZnO film. These estimations are based on the values of the EA signal intensity, V_{EA} , in Fig. 6. Although the values of V_{EA} may have some experimental error, it has at least been confirmed that the ZnO band for $V_{\text{bias}} > 1.5$ V is effectively flat as shown in Fig. 7(b).

In Fig. 7(b), it is illustrated that, for $V_{\text{bias}} > 1.5$ V, a large electric dipole moment is induced at the ZnPc/Au interface and almost all of the applied bias is spent in this region. This is based on our previous results [4, 19] that the ZnPc/Au contact is not ohmic but, when a positive bias is applied to the Au layer, an anomaly occurs at the interface probably due to the accumulation of a large number of negative charges at the surface of the ZnPc layer. This anomaly is attributed to the roughness of the ZnPc/Au interface, which generates a large number of electron traps [19]. At the interface dipole moment, a large electric field should exist. This electric field is not detected by EA,

which may indicate that the dipole is formed on a thin interface layer of unknown origin between ZnPc and Au.

We estimate the voltage drops across the ZnO and ZnPc layers from the resistivities of the layers which are of the order of 10^{-1} and $10^6 \Omega \text{ cm}$, respectively. Using these values, the resistances of the present ZnO and ZnPc layers to the normal direction are calculated to be 10^{-5} and 50Ω , respectively. At $V_{\text{bias}} = 1.5 \text{ V}$, the dark current of the present device with the effective area of 0.3 cm^2 is $15 \mu\text{A}$. Then, the voltage drop across the ZnO and ZnPc layers should be of the order of 10^{-10} and 10^{-3} V , respectively. This is in agreement with the present EA observation that the inner electric fields in the ZnO and ZnPc layers are nearly zero for $V_{\text{bias}} = 1.5 \text{ V}$.

In the present system, the ZnO film is used as an electrode as well as a *n*-type semiconductor. Here, we compare the present ZnO film with an indium-tin-oxide (ITO) film, the latter being the most popular transparent electrode. 1) The sheet resistance of the present ZnO films is $5 \sim 10 \text{ k}\Omega/\square$ which is much higher than that of ITO, a typical value of the latter being $50 \Omega/\square$. 2) The reported values of the work functions of ZnO and ITO are 4.5 and 4.7 eV, respectively [6]. The difference between these values is consistent with the present results: The ZnO/ZnPc/Au cells show rectification indicating the formation of a Schottky barrier, while no rectification is observed for ITO/ZnPc/Au. For the extensive use of ZnO as an electrode, the resistivity of ZnO should be lowered substantially. A study using a Ga-doped ZnO film which has a sheet resistance of $20 \Omega/\square$ is now in progress.

4. Conclusions

The ZnO/ZnPc/Au cell with a ZnO film prepared with a VI/II ratio of 90 shows significantly better rectification and photovoltaic properties compared to the cell with VI/II = 10. The better photovoltaic properties for VI/II = 90 may be due to the existence of unknown impurities or defects that enhance the dissociation of the excitons in the ZnO layer.

For the ZnO/ZnPc/Au cell with VI/II = 90, both the photocurrent action spectrum and the EA spectrum have signals from ZnO but negligibly small or no signals from ZnPc. This indicates that the photocurrent is generated only by the excitation of ZnO and the inner electric field exists only in the ZnO layer. However, no good correlation is seen between the bias dependences of the photocurrent and the inner electric field for the ZnO layer. This indicates that the inner electric field in the ZnO layer does not have any essential role in photocurrent generation. On the other hand, the absence of the photocurrent by the excitation of ZnPc is attributed to the absence of the inner electric field in the ZnPc layer.

References

- [1] J. J. M. Halls, R. H. Friend, in: M. D. Archer, R. Hill (Eds.), Clean Electricity from Photovoltaics, Imperial College Press, London, 2001, Chap. 9.

- [2] J. Nelson, The Physics of Solar Cells, Imperial College Press, London, 2003, p. 137.

- [3] I. Hiromitsu, Y. Murakami, T. Ito, J. Appl. Phys. 94 (2003) 2434.

- [4] I. Hiromitsu, G. Kinugawa, Jpn. J. Appl. Phys. 44 (2005) 60.

- [5] I. Hiromitsu, G. Kinugawa, Synth. Met. 153 (2005) 73.

- [6] T. Shirakawa, T. Umeda, Y. Hashimoto, A. Fujii, K. Yoshino, J. Phys. D: Appl. Phys. 37 (2004) 847.

- [7] T. Umeda, T. Shirakawa, A. Fujii, K. Yoshino, Jpn. J. Appl. Phys. 42 (2003) L1475.

- [8] W. J. E. Beek, M. M. Wienk, M. Kemerink, X. Yang, R. A. J. Janssen, J. Phys. Chem. B109 (2005) 9505.

- [9] J. C. Bernède, H. Derouiche, V. Djara, Sol. Energy Mater. Sol. Cells 87 (2005) 261.

- [10] K. Keis, E. Magnusson, H. Lindström, S. E. Lindquist, A. Hagfeldt, *Sol. Energy Mater. Sol. Cells* 73 (2002) 51.
- [11] T. Minami, H. Tanaka, T. Shimakawa, T. Miyata, H. Sato, *Jpn. J. Appl. Phys.* 43 (2004) L917.
- [12] G. D. Sharma, R. Kumar, S. K. Sharma, M. S. Roy, *Sol. Energy Mater. Sol. Cells* 90 (2006) 933.
- [13] Y. Fujita, R. Nakai, *J. Crystal Growth* 272 (2004) 795.
- [14] I. H. Campbell, T. W. Hagler, D. L. Smith, J. P. Ferraris, *Phys. Rev. Lett.* 76 (1996) 1900.
- [15] D. C. Look, D. C. Reynolds, C. W. Litton, R. L. Jones, D. B. Eason, G. Cantwell, *Appl. Phys. Lett.* 81 (2002) 1830.
- [16] L. Sebastian, G. Weiser, H. Bässler, *Chem. Phys.* 61 (1981) 125.
- [17] P. A. Lane, J. C. deMello, R. B. Fletcher, M. Bernius, *Appl. Phys. Lett.* 83 (2003) 3611.

[18] P. J. Brewer, P. A. Lane, A. J. deMello, D. D. C. Bradley, J. C. deMello, *Adv. Funct. Mater.* 14 (2004) 562.

[19] M. Nonomura, I. Hiromitsu, S. Tanaka, *Appl. Phys. Lett.* 88 (2006) 042111.

[20] H. Sheng, S. Muthukumar, N. W. Emanetoglu, Y. Lu, *Appl. Phys. Lett.* 80 (2002) 2132. Although they do not present the value of the depletion-layer width in the ZnO film, it can be estimated to be ~ 100 nm for $V_{\text{bias}} = 0$ V using the parameter values presented in ref. 20.

Figure Captions

Fig. 1. Scheme of the ZnO/ZnPc/Au sandwich cell and electric circuit for EA measurement.

Fig. 2. PL spectra of the ZnO films for VI/II = 90 (solid line) and 10 (broken line) measured at 15 K. The PL intensity for VI/II = 90 is enlarged by a factor of 15.

Fig. 3. The bias dependences of the current densities of the ZnO/ZnPc/Au cells (a) in the dark and (b) under an illumination of AM 1.5, 100 mW/cm² light, for VI/II = 90 (filled circles) and 10 (open circles).

Fig. 4. (a) Photocurrent action spectra of the ZnO/ZnPc/Au cell for VI/II = 90 measured under $V_{\text{bias}} = 0$ V (solid line) and 0.6 V (broken line), corrected for a light intensity of 1 mW. (b) Optical absorption spectra of the ZnO film for VI/II = 90 (solid line) and a ZnPc film of 50 nm thickness (broken line). (c) EA spectra of the ZnO/ZnPc/Au cell for VI/II = 90 measured under $V_{\text{bias}} = 0$ V (solid line) and 0.6 V (broken line).

Fig. 5. EA spectrum of the ZnO/ZnPc/Au cell for VI/II = 90 with $V_{\text{bias}} = 0$ V (solid line), and the 2nd derivative of the absorption spectrum of the ZnO film (broken line). V_{EA} of ZnO is defined in the figure.

Fig. 6. The bias dependence of the EA signal intensity V_{EA} of ZnO.

Fig. 7. Proposed schematic band structure of the ZnO/ZnPc/Au cell for (a) $V_{\text{bias}} = 0$ V and (b) $V_{\text{bias}} > 1.5$ V.

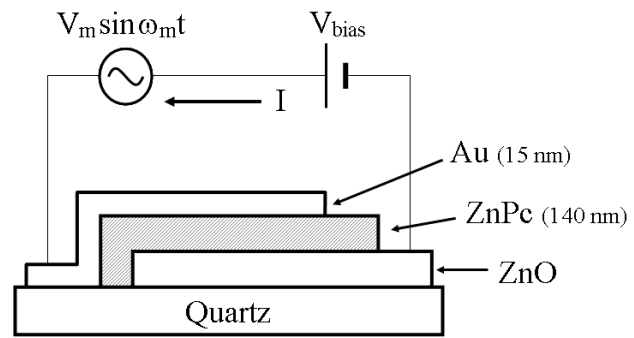


Fig. 1 Y. Yoshida et al.

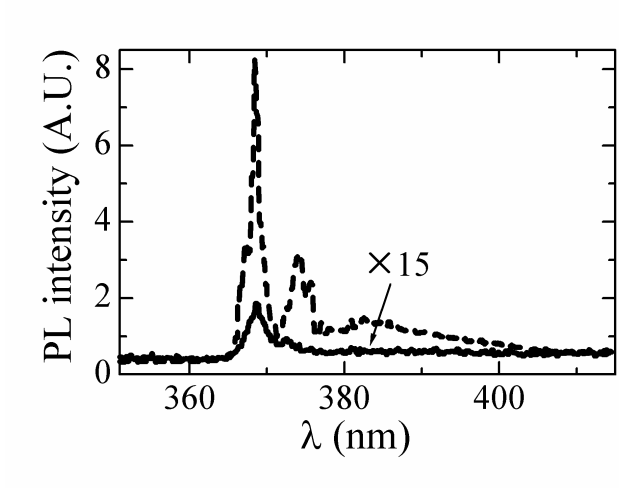


Fig. 2 Y. Yoshida et al.

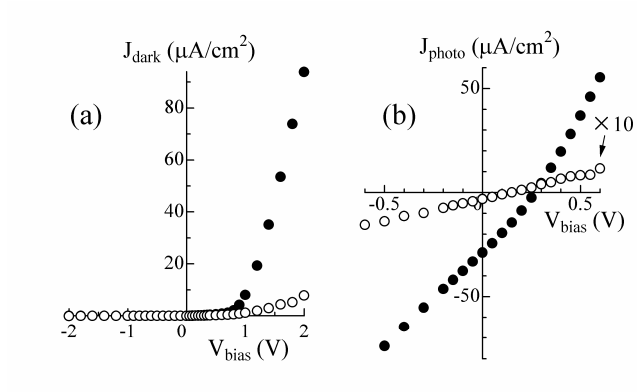


Fig. 3 Y. Yoshida et al.

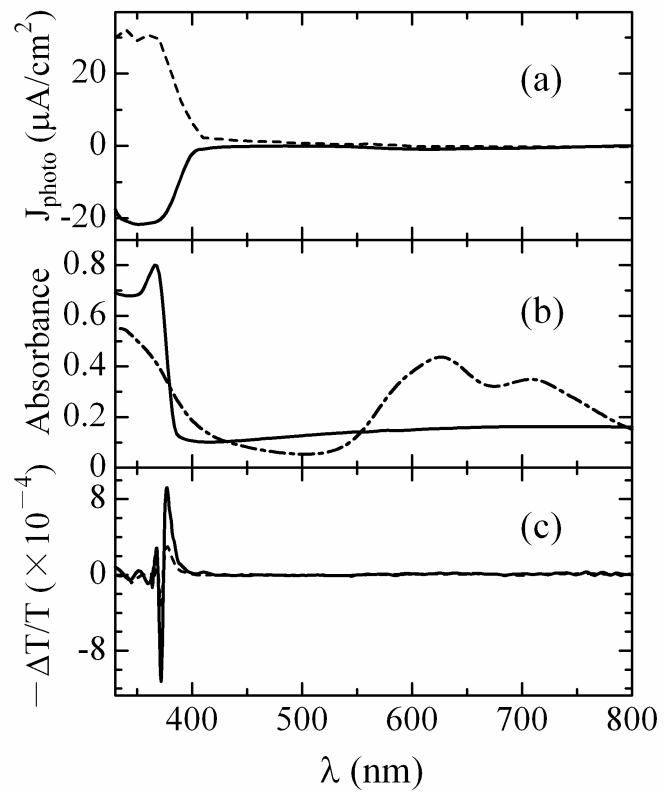


Fig. 4 Y. Yoshida et al.

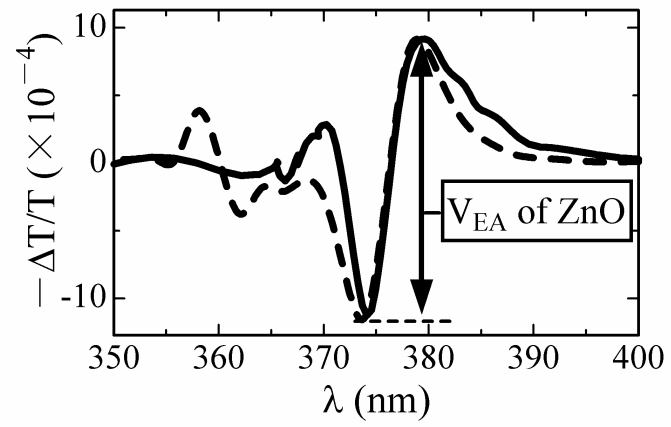


Fig. 5 Y. Yoshida et al.

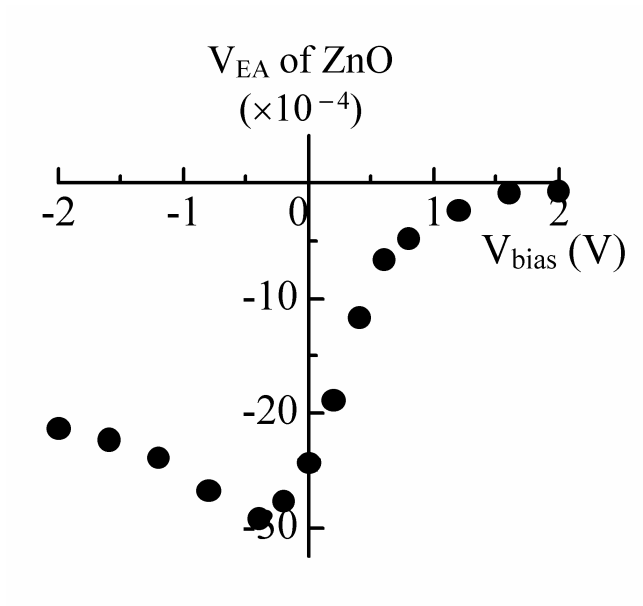


Fig. 6 Y. Yoshida et al.

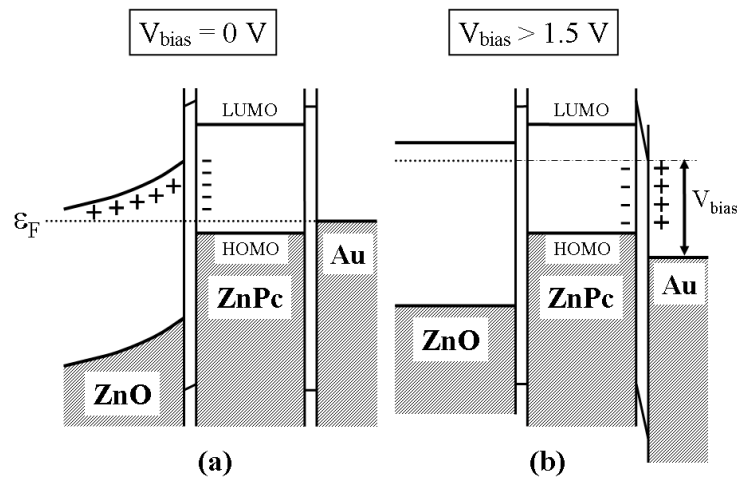


Fig. 7 Y. Yoshida et al.